



## Original article

## Metallation of pentaphyrin with Lu(III) dramatically increases reactive-oxygen species production and cell phototoxicity

Maurizio Ballico<sup>a</sup>, Valentina Rapozzi<sup>b</sup>, Luigi E. Xodo<sup>b,\*\*</sup>, Clara Comuzzi<sup>a,\*</sup><sup>a</sup> Department of Chemical Science, University of Udine, Via del Cotonificio, 108, 33100 Udine, Italy<sup>b</sup> Department of Biomedical Science and Technology, University of Udine, P.le Kolbe, 4, 33100 Udine, Italy

## ARTICLE INFO

## Article history:

Received 16 July 2010

Received in revised form

24 November 2010

Accepted 7 December 2010

Available online 14 December 2010

## Keywords:

Pentaphyrin

Lu(III)

PDT

ROS

Cell proliferation

## ABSTRACT

Photodynamic therapy (PDT) is an emerging cancer treatment modality based on the excitation of a nontoxic photosensitizer with harmless visible light to produce reactive-oxygen species (ROS) that induce apoptosis and/or necrosis in cancer cells. As the efficacy of this therapy strongly depends of the nature of the photosensitizer, there is a great interest to develop new photoactive molecules. Here we report for the first time the synthesis, characterization and bioactivity of metal complexes between the non-aromatic expanded porphyrin, namely 20-[[4'-(Trimethylsilyl)ethoxycarbonyl]phenyl-2,13-dimethyl-3,12-diethyl-[24] iso-pentaphyrin (PCRed) and Zn(II) [Zn(II)-PCRed] or Lu(III) [Lu(III)-PCRed]. The complexation of these two diamagnetic heavy metal ions to PCRed improved the properties of the free photosensitizer as a PDT drug. We discovered that the 1:1 complex between PCRed and Lu(III) significantly increases the cellular uptake, ROS production and antiproliferative capacity in four cancer cell lines. Our study shows that metal complexation is a useful strategy to potentiate iso-pentaphyrin as a PDT drug.

© 2010 Elsevier Masson SAS. All rights reserved.

## 1. Introduction

Large polypyrrole macrocycles or expanded porphyrins, composed by five or more pyrrole rings, are versatile ligands capable to coordinate almost all metals and semimetals of the periodic table [1] and act as receptors of anions [2] or neutral molecules [3]. Expanded porphyrins may be used for a wide range of applications including lanthanide and actinide complexation [4], anion binding and optics [1,5], biomedical applications as magnetic resonance imaging [4] (MRI, paramagnetic contrast agents), anti-sense-targeted RNA [6], X-ray radiation sensitization [4g] and visible-light-based photodynamic therapy (PDT) [7]. PDT is a local treatment designed to eliminate abnormal tissue lesions including cancer [8]. It requires the administration to the tumor tissue of a photosensitizer agent, which becomes active when it is irradiated with light. The activated photosensitizer transfers energy to molecular oxygen to generate reactive-oxygen species (ROS), in particular singlet oxygen, that causes cell death [9]. A macrocycle that strongly adsorbs in the region where the body is most

transparent and efficiently generates ROS and singlet oxygen (<sup>1</sup>O<sub>2</sub>) is a potential PDT agent. The photosensitizer most widely used in clinic is Photofrin, a defined mixture of haematoporphirin [8]. However, in the last decade many new compounds have been produced and tested and nowadays PDT has the potential to become a major treatment in cancer therapy. Among these new drugs, expanded porphyrins have been successfully tested as PDT photosensitizers [10]. Expanded porphyrins of the type [1.1.1.1], called pentaphyrins, have been not thoroughly investigated. These compounds contain five pyrrolic rings linked by means of meso-like bridges, which make the macrocycle flexible and capable of assuming different conformations. We have previously reported the synthesis and photosensitizing properties of two [1.1.1.1]-macrocycles characterized by a different oxidation state: non-aromatic iso-pentaphyrin with 24 π-electrons and aromatic pentaphyrin with 22 π-electrons [11]. To improve their phototoxicity we decided to coordinate the pentaphyrin macrocycle to diamagnetic metal ions. We reasoned that the insertion of a metal into the central core of the expanded porphyrin should produce two main effects: the shift of the absorption peaks to longer wavelengths, i.e. into the ideal spectral region (650–800 nm) and an increased production of ROS and <sup>1</sup>O<sub>2</sub> due to heavy metal effects. In fact, the presence of a central metal ion can strongly influence the photokilling efficiency of a photosensitizer [10b, 12]. To

\* Corresponding author. Tel.: +39 0432 558823; fax: +39 0432 558803.

\*\* Corresponding author. Fax: +39 0432 494301.

E-mail addresses: [luigi.xodo@uniud.it](mailto:luigi.xodo@uniud.it) (L.E. Xodo), [clara.comuzzi@uniud.it](mailto:clara.comuzzi@uniud.it) (C. Comuzzi).

understand the heavy metal effect, one should consider the mechanism of singlet oxygen formation. Upon activation, the photosensitizer is promoted from its ground state ( $S_0$ ) to the first excited singlet state ( $S_1$ ) from which it can change its spin multiplicity to a triplet excited state ( $T_1$ ) through intersystem crossing (ISC). Energy transfer to triplet oxygen to yield highly reactive singlet oxygen occurs when the triplet state of the photosensitizer is significantly populated. The efficiency of singlet oxygen production [13] is directly related to the quantum yield of triplet state of the photosensitizer and its lifetime. In this mechanism ISC is a key parameter. Some diamagnetic metals are known to enhance ISC and to elongate triplet lifetime of the photosensitizer. For the series of diamagnetic metals including Y, In, Lu and Cd, the production of singlet oxygen was found proportional to the increase in atomic number: a result that is interpreted as a heavy atom effect [14]. Instead, paramagnetic species deactivate the excited state, reduce the excited-state lifetime and prevent photochemical reactions from taking place [13]. In fact, it has been demonstrated that photophysical parameters that are directly associated with the intrinsic decay rates of the singlet excited state or fluorescence lifetimes, are enhanced by coordination of paramagnetic metal ions. So, the coordination of paramagnetic metals to photosensitizers decreases the singlet oxygen production. However, there are exceptions to this general behavior especially revealed for porphyrins and phthalocyanines [10b,12,13].

Here we describe the synthesis of two new macrocycles belonging to the class of [1.1.1.1.1]-pentaphyrins, namely the partially oxidized pentaporphynogen **3** and the non-aromatic PCRed **4** (with 24  $\pi$ -electrons) (Scheme 1).

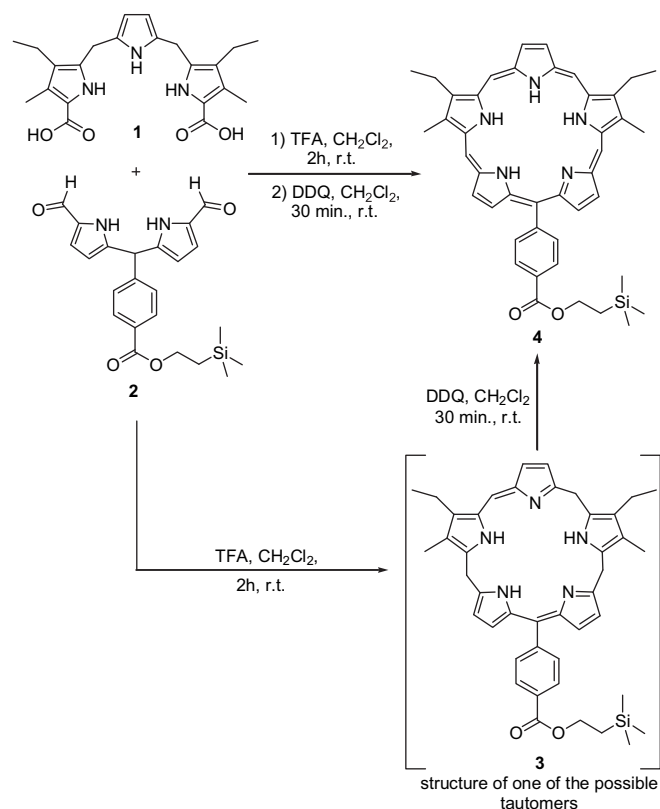
We have modified the original structure of the pentaphyrins by replacing the diethyl-pyrrole with an unsubstituted pyrrole and by introducing a carboxylic group on the phenyl substituent. These two changes were made to eliminate the time-consuming synthesis of 3,4-diethyl-pyrrole, improve the solubility in polar solvents of these molecules and allow the conjugation of PCRed with polyethylene glycol (PEG) to obtain a photosensitizer with a superior bioavailability. To study the heavy metal effect on PCRed we coordinate it to Zn(II) and Lu(III) (**5**, **6**) (Schemes 2 and 3). The new compounds have been characterized by spectroscopic analyses, while the stoichiometry of the complexes was determined by mass spectrometry (ESI-MS and EI). The biological activity of these new compounds was tested in four different cell lines in terms of ROS production and phototoxicity.

## 2. Results and discussion

### 2.1. Synthesis and characterization of the PCReds

The synthesis of PCRed **4** was performed following a modified McDonald-type acid-catalyzed [3 + 2] condensation strategy as shown in Scheme 1 [11]. PCRed was obtained as a green metallic film in 50% yield and characterized by a combination of ESI mass spectrometry, NMR and UV–vis spectroscopy.  $^1\text{H}$  NMR of **4** in  $\text{CD}_3\text{OD}$  shows the non-aromatic character of this molecule: meso-CH are detected at  $\delta$  6.52 and 5.60 ppm,  $\text{CH}_2$  quartet of the ethyl substituents appears at  $\delta$  3.13 ppm, while the singlet methyl resonance at  $\delta$  1.20 ppm. In the  $\text{CDCl}_3$  spectrum, NH protons were detected at  $\delta$  11.41, 10.21 and as a large signal in the region from 8.80 to 8.10 ppm (overlapped to the aromatic signals); the absence of upfield shift of the nitrogen protons indicate the lack of a large diamagnetic ring current characteristic of aromatic porphyrins.

The (+)-ESI mass spectrometry studies confirmed the proposed structure for **4** and showed that this macrocycle can form complexes with small neutral molecules: depending on sample preparation, peaks in the mass spectrograms corresponding to both



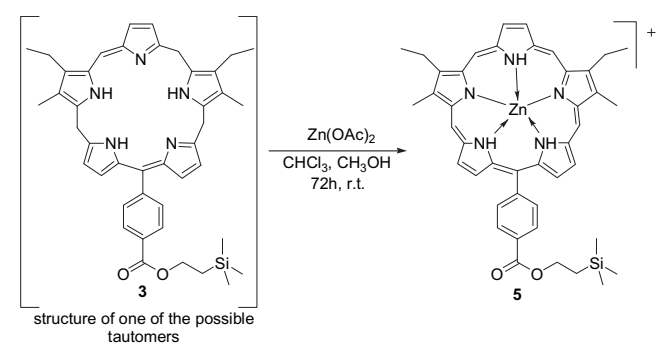
**Scheme 1.** Synthesis of the PCRed **4**, and the partially oxidized pentaporphynogen **3**.

water and methanol adducts could be seen ( $m/z$  712 ( $[\text{MH} + \text{H}_2\text{O}]^+$ ) and 726 ( $[\text{MH} + \text{CH}_3\text{OH}]^+$ ). Finally the UV–vis spectrum recorded in  $\text{CH}_2\text{Cl}_2$  exhibits a strong Soret-like band at 485 nm ( $\log \epsilon = 4.39$ ) and a Q-band at 814 nm ( $\log \epsilon = 3.71$ ) (Supporting information S1).

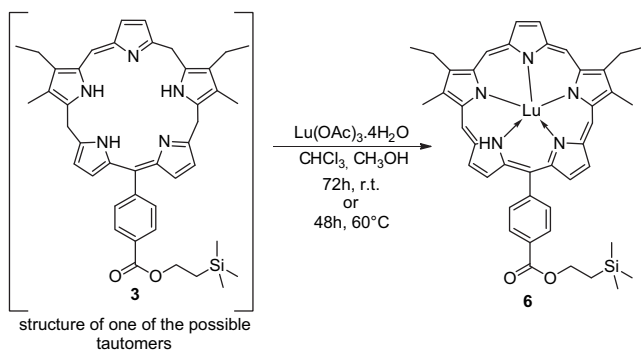
Partially oxidized pentaporphynogen **3** was obtained following a modified McDonald-type acid-catalyzed [3 + 2] condensation seen for **4**, but the oxidation step with DDQ was omitted and the workup of the molecule was performed at the end of the cyclization. Compound **3** was isolated to investigate the mechanism of [3 + 2] cyclization and successive macrocycle oxidation, to synthesize a highly flexible molecule able to coordinate metal ions of different dimension more easily than oxidized pentaphyrins.

The (+)-ESI-MS spectrum (in  $\text{CH}_3\text{OH}$ ) displays the protonated molecular ion peak at  $m/z$  696 ( $[\text{MH}]^+$ ), suggesting the presence of a reduced form of the pentaphyrin and adducts with  $m/z$  714 ( $[\text{MH} + \text{H}_2\text{O}]^+$ ) and 728 ( $[\text{MH} + \text{CH}_3\text{OH}]^+$ ).

The complexity of the  $^1\text{H}$  NMR spectrum reveals that the partially oxidized pentaporphynogen **3** is a very flexible macrocycle



**Scheme 2.** Simultaneous oxidation/metallation of the partially oxidized pentaporphynogen **3** with zinc acetate: synthesis of the Zn(II)-PCRed **5**.



**Scheme 3.** Simultaneous oxidation/metallation of the partially oxidized pentaporphyrinogen **3** with Lutetium acetate hydrate: synthesis of the Lu(III)–PCRed **6**.

that exists in solution in several rapidly exchanging tautomers and conformers with comparable stability. None of these structures is fully conjugated. We identified multiple peaks attributable to the same protons in different isomers where the macrocycle conjugation is interrupted. For example, the  $^1\text{H}$  NMR spectrum in  $\text{CDCl}_3$  showed several signals in the region between  $\delta$  12.0 and 10.0 ppm due to exchanging NH protons and various doublets attributable to the  $\beta$ -pyrrolic protons of the isomers in the region between  $\delta$  6.0 and 8.0 ppm.

The UV–vis spectrum in  $\text{CH}_2\text{Cl}_2$  displays two large bands at 300 nm ( $\log \epsilon = 4.16$ ) and 482 nm ( $\log \epsilon = 4.21$ ), and a single broad Q-type band at 802 nm ( $\log \epsilon = 3.93$ ). Interestingly, the intensity of the Q-type band is greater in compound **3** than in **4**. The partly oxidized pentaporphyrinogen **3** was converted into **4** by using DDQ as an oxidizing agent. It is interesting to note that the [3 + 2] condensation did not give the pentaporphyrinogen, but only a more stable oxidized macrocycle (partly oxidized pentaporphyrinogen **3**). The fluorescence spectrum of **4** in methanol shows a broad emission band between 500 and 550 nm, with a maximum around 540 nm ( $\text{Ex } 480 \text{ nm}$ ) (Supporting information S2). Its intensity is indirectly proportional to pentaphyrin concentration (from  $1.78 \times 10^{-5} \text{ M}$  to  $5.18 \times 10^{-7} \text{ M}$ ). In  $\text{CH}_2\text{Cl}_2$  the fluorescence spectrum does not change, showing a broad band with a maximum at 525 nm ( $\lambda_{\text{ex}} = 480 \text{ nm}$ ) but, in this case, the intensity is directly proportional with concentration (from  $5.74 \times 10^{-7} \text{ M}$  to  $1.78 \times 10^{-5} \text{ M}$ ).

## 2.2. Metallation chemistry of PCReds

The size of the central cavity of PCRed is expected to be similar to that of sapphyrin ( $\sim 5.5 \text{ \AA}$ ). Compared to porphyrins, the presence of an additional nitrogen donor allows this molecule to act as a pentadentate ligand, potentially capable of coordinating a plethora of metal cations. To investigate the effects of heavy metals we synthesized complexes between PCRed and Zn(II) and Lu(III). We used these metal ions because diamagnetic Zn(II) coordinated to phthalocyanines and porphyrins strongly increased their photosensitizing property [15]; while Lu(III) having a higher atomic weight provides a good system to investigate the heavy metal effect. It should be remembered that LuTex is one of the most efficient photosensitizers known up to date [16].

PCRed–metal complexes were synthesized by direct reaction between Zn(II) or Lu(III) and **4**. However, a simplified synthetic route allows to insert, by simultaneous oxidation and metallation reactions, the metals on **3** and to obtain complexes **5** and **6**. The treatment in air of **3** dissolved in  $\text{CHCl}_3$  with an excess of anhydrous Zn(II) acetate in  $\text{CH}_3\text{OH}$ , at room temperature for 48 h, resulted in the formation of complex **5**, which was characterized by UV–vis spectroscopy,  $^1\text{H}$  NMR, 2D COSY and NOESY measurements. The stoichiometry of the complex was established by mass spectrometry.

The (+)-ESI-MS spectrum in  $\text{CH}_3\text{OH}$  of **5** shows the molecular ion peak at  $m/z$  756 ( $[\text{M}]^+$ ) (Supporting information S3), which was identified to be a 1:1 complex between Zn(II) and PCRed **4** (Scheme 2). The ESI-MS spectrum of **5** shows signals at  $m/z$  774 and 788 corresponding to adducts with  $\text{H}_2\text{O}$  and  $\text{CH}_3\text{OH}$ , respectively. The addition of formic acid (0.2%) to a solution of **5** in MeOH resulted in a rapid demetallation. Indeed, (+)-ESI-MS mass spectrum of this solution reveals the complete disappearance of the peaks relative to the complex and the appearance (as main peaks) of the signals attributable to the PCRed **4** (in particular peaks at  $m/z$  694 ( $[\text{MH}]^+$ ) and 726 ( $[\text{MH} + \text{CH}_3\text{OH}]^+$ ). This is a further evidence that, during the synthesis of **5**, the coordination of the metal occurs together with the oxidation of the macrocycle. The  $^1\text{H}$  NMR spectrum of **5** in  $\text{CD}_3\text{OD}$  shows that the coordination of Zn(II) does not cause drastic changes in the pentaphyrin structure: the only signal that undergoes a downfield shift is the meso-CH from  $\delta$  6.52 (**4**) to 7.97 (**5**) ppm, while  $\beta$ -pyrrolic, phenylic and other meso-CH protons do not change. This simple NMR pattern suggests that the symmetry of the macrocycle is retained by the complexation of the zinc ion (Supporting information S4, S5). The signals of the alkyl substituents in  $\beta$ -position are those most affected by complexation: the quartet of the ethyl- $\text{CH}_2$  protons was downfield shifted from  $\delta$  3.16 to 4.10 ppm and singlet  $\text{CH}_3$  from  $\delta$  1.26 to 2.05 ppm. This indicates that the pyrroles are directly involved in the coordination to Zn(II). The absence in 2D NMR NOESY spectra of any correlation between meso-CH and  $\beta$ -pyrrolic protons is a further indication of the high distortion from planarity of this complex. The  $^1\text{H}$  NMR spectra of complex **5** in  $\text{CDCl}_3$  suggest the existence of a mixture of isomeric structures rapidly exchanging on the NMR time scale. The spectrum shows the NH of **5** centered at  $\delta$  10.03 (1H) and 8.0 (2H) as broad signals. NMR and mass spectra indicate that **4** loses only one proton upon complexation with Zn(II), as previously observed [14]. Finally, the UV–vis Soret band of Zn(II)–PCRed **5** in  $\text{CH}_2\text{Cl}_2$  is bathochromatically shifted at 491 nm ( $\log \epsilon = 4.33$ ), while the Q-band is at 817 nm ( $\log \epsilon = 3.37$ ) (Supporting information S1).

We also inserted Lu(III) into **3** using conditions similar to those used for the complexation of Zn(II). We used  $\text{Lu}(\text{OAc})_3 \cdot 4\text{H}_2\text{O}$  and  $\text{Lu}(\text{NO}_3)_3 \cdot 5\text{H}_2\text{O}$  and performed the reactions in THF or  $\text{CHCl}_3/\text{CH}_3\text{OH}$  mixtures, either at room temperature or at  $60^\circ\text{C}$  (Scheme 3). EI-MS spectra show that PCRed **4** forms with Lu(III) a 1:1 complex (**6**). The  $^1\text{H}$  NMR spectra of **6** are similar to those obtained for **5**.  $\text{CD}_3\text{OD}$  spectra show that meso-CH protons appear at  $\delta$  7.81 and 5.60 ppm,  $\beta$ -pyrrolic signals at  $\delta$  9.29, 6.88 and 5.90 ppm;  $\text{CH}_2$  of ethyl groups and singlet  $\text{CH}_3$  are detected at  $\delta$  3.23 and 1.20 ppm respectively. The  $^1\text{H}$  NMR spectrum of **6** in  $\text{CDCl}_3$  shows only one NH signal at 9.83 ppm (1H). The others NH signals at 11.41 ppm (1H), 10.21 ppm (1H) and 8.80–8.10 ppm (overlapped to the aromatic signals) disappeared from the spectrum upon Lu(III) complexation. This result suggests that the coordination of Lu(III) causes the ligand to lose three protons leading to a neutral complex. This is the reason why we could not follow the metal complexation by ESI-MS. The treatment with formic acid produces a partial demetallation of the complex which releases free PCRed **4**. This reaction was easily followed by ESI-MS as in the spectrum appeared the characteristic peaks of **4** at  $m/z$  694 ( $[\text{MH}]^+$ ) and 726 ( $[\text{MH} + \text{CH}_3\text{OH}]^+$ ). The UV–vis spectrum of complex **6** in  $\text{CH}_2\text{Cl}_2$  (Supporting information S1) shows a pattern completely different from that of complex **5**, Zn(II)–PCRed, with broad bands between 300 and 600 nm: at 339 nm ( $\log \epsilon = 4.25$ ), at 406 nm ( $\log \epsilon = 4.15$ ) and at 498 nm ( $\log \epsilon = 3.99$ ). These bands are blue shifted compared to **5** and this can be ascribed to the formation of aggregates in this solvent [17]. However, the addition of small amount of TFA to complex **6** in dichloromethane causes the appearance of the Soret band at 480 nm (Supporting information S1 insert). Complexes **5** and **6** show broad fluorescence emission spectra in the region between

500 and 550 nm, when excited at 480 nm (Supporting information S6 and S7). Fluorescence spectra of the Lu(III)–PCRed **6** shows two peaks at 518 and 558 nm in methanol (Ex 480 nm). Instead, in PBS buffer the fluorescence emission of **5** and **6**, in the region between 500 and 550 nm, is quenched and comparable to that of **4** in the same medium.

### 2.3. Phototoxicity of metallated PCRed

To evaluate the photosensitizing activity of the PCRed–metal complexes we first investigated their uptake in B78-H1 cells (Fig. 1). We found a clear dependence of the cellular uptake from the charge of the metal complexes. As PCRed **4**, upon excitation at 488 nm, emits green fluorescence, we measured by flow cytometry (Fig. 1a) the fluorescence of B78-H1 cells treated for 24 h with PCRed **4** or its

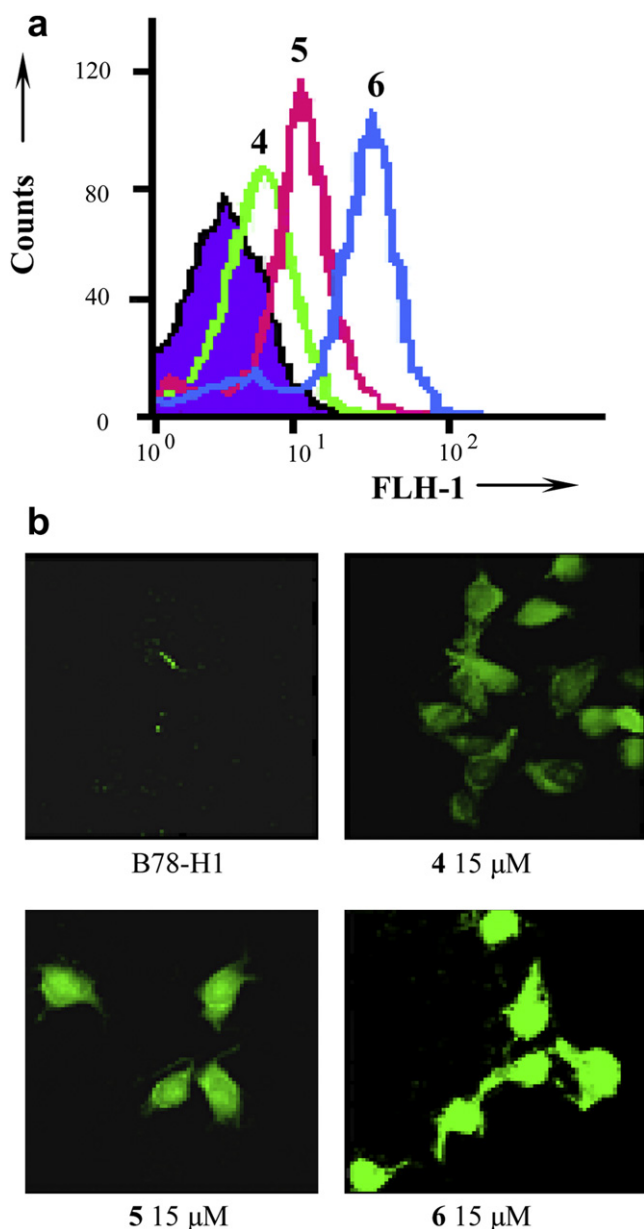


**Fig. 1.** (a) Cell cytometry of B78-H1 cells treated with 15  $\mu\text{M}$  compounds **4**, **5** and **6**. Fluorescence of cells treated with **4**, **5** and **6** is 8, 10 and 40 FU, respectively; (b) Confocal microscopy images of B78-H1 cells treated with **4**, **5** and **6**. Ex. 488 nm (Arg laser); Em. 500–530 nm.

metal complexes **5** and **6** (15  $\mu\text{M}$ ). It can be seen that the fluorescence associated with the cells treated with **4**, **5** and **6** was 8, 10 and 40 FU, respectively. These results show that all three PCReds have the capacity to penetrate the cell membrane, but the complexation to Zn(II) and Lu(III) significantly increases the uptake. The higher uptake of **6** compared to **5** can be rationalized by considering that Lu(III)–PCRed is a neutral compound, while Zn(II)–PCRed is a cationic species. Neutral molecules being more lipophilic are expected to penetrate the cell membrane easier than charged molecules. In order to investigate the intracellular distribution of the PCReds, we performed confocal laser microscopy experiments with B78-H1 cells. Fig. 1b shows the green fluorescence emitted by the cells treated with **4**, **5** and **6**. The fluorescence distribution suggests that the two metal complexes locate in both the nucleus and cytoplasm, probably with a slight preference for the latter. Instead, PCRed **4** appears clearly more localized in the cytoplasm, in keeping with previous data obtained with HeLa cells [11a]. The decrease of fluorescence intensity from **6** to **4** correlates with the flow cytometry data showing that the decrease of uptake follows the order  $6 > 5 > 4$ .

The photodynamic effect promoted by the complexes between PCRed and Zn(II) or Lu(III) was tested in four cancer cell lines: B78-H1 murine melanotic clone derived from melanoma B16; HeLa human cervix adenocarcinoma; HepG2 human hepatic carcinoma and MCF-7 human breast cancer. Fig. 2 shows that in HeLa and B78-H1 cells, compounds **4**, **5** and **6** are basically not

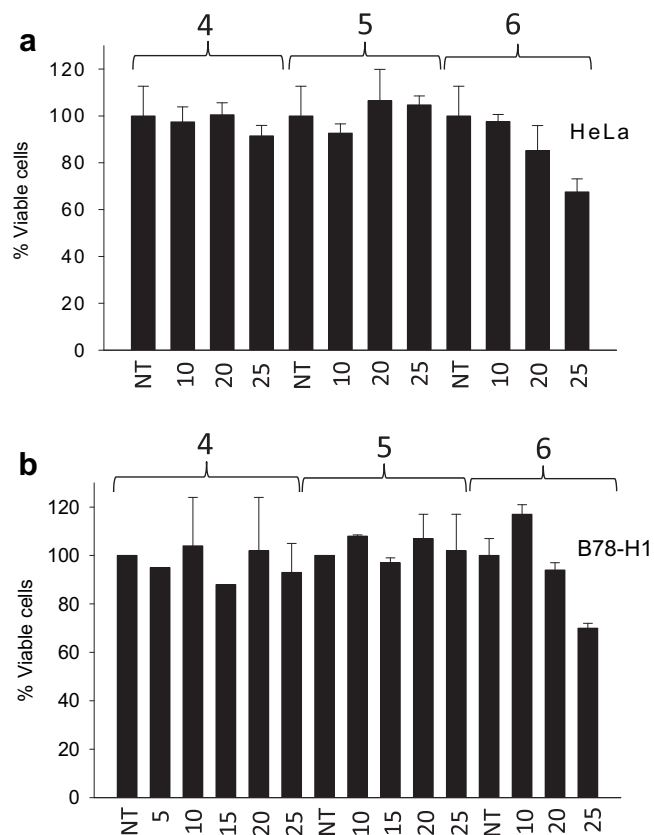


**Fig. 2.** Cytotoxicity in the dark of compounds **4**, **5** and **6** in HeLa (a) and B78-H1 (b) cells. Numbers below bars indicate pentaphyrin concentrations ( $\mu\text{M}$ ); NT means pentaphyrin untreated cells. Numbers at top bars indicate the pentaphyrin used in the treatment (**4**, **5** or **6**). Viable cells were measured with resazurin. Histograms report in ordinate the percent of viable cells, i.e. the ratio  $\text{RFU}_T/\text{RFU}_C \times 100$ , where  $\text{RFU}_T$  is the fluorescence of treated cells, while  $\text{RFU}_C$  is the fluorescence of untreated cells. The data are the means  $\pm$  sd of three experiments.

cytotoxic in the dark, up to 25  $\mu\text{M}$  (**4** and **5**) or 20  $\mu\text{M}$  (**6**). A similar result was obtained with the MCF-7 and HepG2 cells (data not shown).

When PCRed **4** is irradiated with a halogen light at a fluence of 8  $\text{mW}/\text{cm}^2$  (14  $\text{J}/\text{cm}^2$ ), a slight cytotoxic effect is promoted at photosensitizer concentrations higher than 25  $\mu\text{M}$  (Figs. 3 and 4). In contrast, the two metal complexes **5** and **6** displayed, after irradiation, a stronger cytotoxic effect proportional to the atomic weight of the metal ion (Lu(III)-PCRed **6** > Zn(II)-PCRed **5**) [10,13]. These experiments were carried by treating the cells for 24 h with increasing amounts of photosensitizer, followed by irradiation and 24 h-incubation in the dark before a resazurin proliferation assay was performed. As a control the cells were treated with the same amount of DMSO present in the PCReds treatment (PCReds were dissolved in DMSO and diluted with cell medium). From these plots we estimated the  $\text{IC}_{50}$  values reported in Table 1. These values show that free PCRed **4** has little if no photoactivity. But when it is coordinated to Zn(II), its light-induced cytotoxicity slightly improved. In contrast, the complexation of PCRed with Lu(III) dramatically increases the phototoxicity of complex **6**, for which we found a  $\text{IC}_{50}$  between 5 and 12  $\mu\text{M}$  (values comparable to those found for the previously tested aromatic pentaphyrin analogues [11]).

In order to evaluate the photokilling mechanism triggered by the photoactivated PCReds we measured in B78-H1 cells the levels of ROS production 24 h after light activation. To this purpose we carried out a standard CM-H<sub>2</sub>DCFDA assay based on the observation that the dye in its reduced form is not fluorescent, but it becomes so when it is oxidized by ROS and the dye acetate groups are removed by cellular esterases [18].

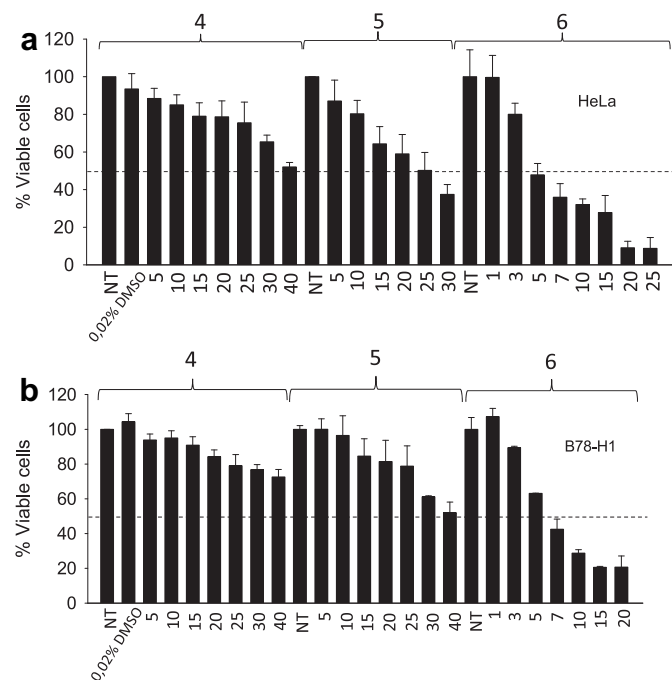


**Fig. 3.** Phototoxicity of PCReds (**4**, **5** and **6**) in HeLa and B78-H1 cells. % Viable cells in samples treated with increasing amounts of pentaphyrin after light treatment (fluence 14  $\text{J}/\text{cm}^2$ ). Viable cells were measured with resazurin. Histograms report in ordinate the percent of viable cells, i.e. the ratio  $\text{RFU}_T/\text{RFU}_C \times 100$ , where  $\text{RFU}_T$  is the fluorescence of treated cells, while  $\text{RFU}_C$  is the fluorescence of untreated cells. The data are the means  $\pm$  sd of three experiments. Numbers below the bars indicate pentaphyrin concentrations ( $\mu\text{M}$ ); NT means pentaphyrin untreated cells. Numbers at top of the bars indicate the pentaphyrin used in the treatment (**4**, **5** or **6**).

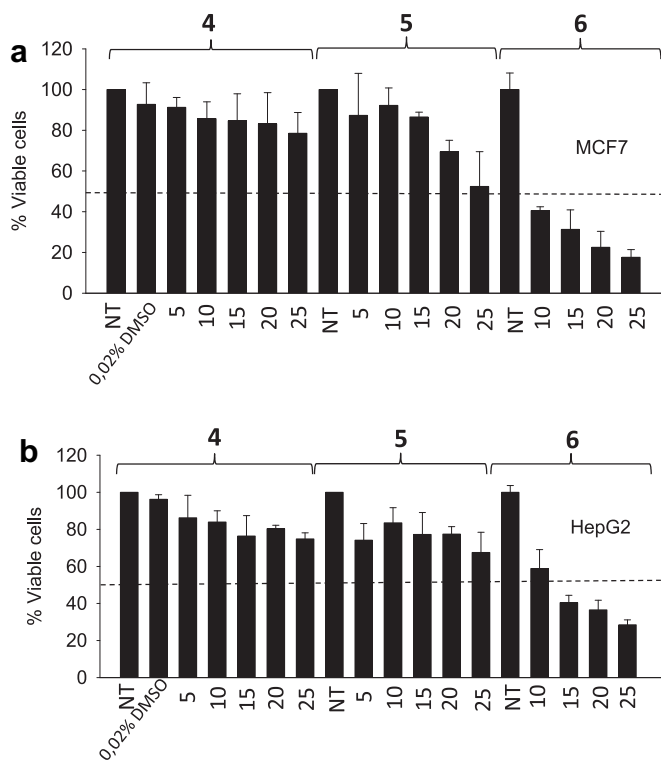


**Fig. 4.** Phototoxicity of PCReds (**4**, **5** and **6**) in MCF-7 and HepG2 cells. % Viable cells in samples treated with increasing amounts of pentaphyrins after light treatment (fluence 14  $\text{J}/\text{cm}^2$ ). Viable cells were measured with resazurin. Histograms report in ordinate the percent of viable cells, i.e. the ratio  $\text{RFU}_T/\text{RFU}_C \times 100$ , where  $\text{RFU}_T$  is the fluorescence of treated cells, while  $\text{RFU}_C$  is the fluorescence of untreated cells. The data are the means  $\pm$  sd of three experiments. Numbers below the bars indicate pentaphyrin concentrations ( $\mu\text{M}$ ); NT means pentaphyrin untreated cells. Numbers at top of the bars indicate the pentaphyrin used in the treatment (**4**, **5** or **6**).

The amount of fluorescence generated in the cells by the dye, which is directly proportional to the ROS production, was measured by FACS. The results obtained are in nice accord with the trend observed on measuring the phototoxicity. The Lu(III)-PCRed **6** produces higher ROS levels than Zn(II)-PCRed **5** and PCRed **4** (Fig. 5). The amount of fluorescence generated in the cells by the dye, which is directly proportional to ROS production, was measured. It is worth to note that immediately after irradiation ROS levels of **5** and **6** are similar while after 24 h the production of ROS increased 8-fold with complex **6** and only 3-fold with **5**.

The free ligand **4** produces very low levels of ROS, either immediately or 24 h after irradiation. The data show that metalated PCReds generate ROS with a slow rate, with an efficiency proportional to the atomic weight of the metal cation.

It is worth noting that the insertion of Lu(III) into the macrocycle transforms a compound that does not have any phototoxic activity into an efficient photosensitizer. No structural changes of the complexes can be invoked to explain this effect, as NMR data show no relevant structural diversity between **6** and **5** (in methanol)

**Table 1**  
 $\text{IC}_{50}$  values of compounds **4**, **5** and **6**.

Cells	PCRed <b>4</b> ( $\mu\text{M}$ )	Zn(II)-PCRed <b>5</b> ( $\mu\text{M}$ )	Lu(III)-PCRed <b>6</b> ( $\mu\text{M}$ )
HeLa	40	25	5
B78-H1	>30	40	6
HEPG2	>30	>25	11
MCF-7	>25	25	12

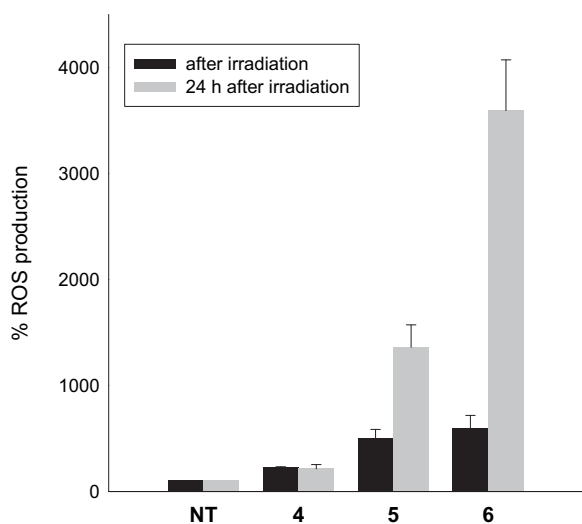


**Fig. 5.** Fluorescence measured by cell cytometry of B78-H1 cells treated for 24 h with pentaphyrin concentrations near  $IC_{50}$  (30  $\mu$ M for **4**; 25  $\mu$ M for **5**; 3  $\mu$ M for **6**), activated with light and treated with 10  $\mu$ M CM-H<sub>2</sub>DCFDA immediately after activation or after 24 h. The increase of fluorescence is proportional to ROS production.

except for the degree of deprotonation of the ligand due to coordination of the metal ion. As the stability of these compounds in physiological conditions was similar over a period of 48 h, the lower activity of **5** compared to **6** cannot be ascribed to demetallation of the complex. So, could this difference in activity be attributed to the fact that complex **6** is taken up by the cells more efficiently than **4** or **5**? This is unlikely because the experiment of Fig. 5 was performed with concentrations of **5** and **6** close to their  $IC_{50}$  values. In fact, the much higher production of ROS by **6** was observed at a concentration 8-fold lower than that of **5**.

However, another phenomenon can account for the different bioactivity of the PCReds. We found that ROS in B78-H1 cells are produced with a slow rate, suggesting that the photodynamic process, triggered by **5** and **6**, is neither of Type I nor of Type II, as these are fast [10a,19]. These mechanisms have been proposed for photosensitizers in their final oxidation state (porphyrins, phthalocyanines, etc). In our systems we were able to rule out a Type II mechanism by means of a 9,10-dimethylanthracene test [20] (Supporting information S8) which demonstrated that compound **4** and **6** did not produce singlet oxygen by irradiation. Therefore, the ROS production has to be ascribed to an electron transfer process triggered by light, consistent with the fact that PCReds molecules are in an intermediate oxidation state [11,21,22]. So, the increase of the PDT effect caused by the coordination of a heavy metal to the macrocycle cannot be due to an enhanced ISC, as currently reported [10,12–14]. Instead, it is likely related to a variation of the oxidation potential within the complexes. These new features induced by metallation open a new approach in the design of efficient photosensitizers based on reduced-state expanded porphyrins.

### 3. Conclusion

In this study we describe a simple synthetic route to obtain metal complexes of pentaphyrin with Zn(II) and Lu(III). These complexes have been characterized by a number of techniques. We found that metallation strongly affects the photosensitizing property of the PCRed. While the free ligand (PCRed) did not show any PDT activity in four cancer cell lines, the Lu(III)-complex promoted a strong PDT effect with an  $IC_{50}$  as low as 5–6  $\mu$ M in HeLa and

B78-H1 cells. The phototoxicity nicely correlates with the higher capacity of the Lu(III)-complex **6** to generate ROS species compared to free PCRed **4** and Zn(II)-PCRed **5**. Metallation is a suitable strategy to potentiate reduced pentaphyrins as PDT drugs.

## 4. Experimental section

### 4.1. General remarks

All solvents and chemicals were of reagent grade quality and were used as received from the suppliers. Mass spectra were recorded on an ion trap Finnigan Mat GCQ (Finnigan MAT, Austin, Texas, USA), operated in electron ionization mode, and on a Finnigan LXQ linear ion trap Mass Spectrometer (Thermo Scientific, Waltham, MA, USA) equipped with an ESI source. Experiments were carried out in the positive ion mode. EI mass spectrums were performed on a Micro-mass VG 7070 H Mass Spectrometer operating at 70 eV (Micromass Ltd., Manchester, UK). Purifications were conducted on a VersaFlash station (Supelco, 595 North Harrison Road, Bellefonte, PA (USA)), supplied with semipreparative VersaPak Cartridges (23  $\times$  53 mm, running at 5 mL/min, Supelco, 595 North Harrison Road, Bellefonte, PA (USA)) containing multiuse end-capped C18 resin (20–45  $\mu$ m particle size), and eluted with water/acetonitrile 1:1 and 1% TFA. <sup>1</sup>H NMR spectra were recorded on a Bruker AM-200 (200 MHz). Chemical shifts are given in ppm ( $\delta$ ) relative to tetramethylsilane (<sup>1</sup>H NMR) as an internal standard. UV–vis spectra were measured on a Varian Cary 50 (Palo Alto, CA, USA) spectrophotometer using 1.0 cm quartz cuvettes. Fluorescence emission spectra were recorded on a spectrofluorometer LS 50B Perkin Elmer in CH<sub>3</sub>OH, CH<sub>2</sub>Cl<sub>2</sub> and PBS in standard quartz cells using a  $\lambda_{exc}$  = 480 nm.

### 4.2. Synthesis of photosensitizers

#### 4.2.1. Synthesis of the partially oxidized pentaporphynogen **3**

100 mg (0.25 mmol) of the tripyrrane diacid **1** was dissolved in 200  $\mu$ L (2.60 mmol) of TFA and stirred for 10 min at room temperature under N<sub>2</sub>. The mixture was diluted with dry CH<sub>2</sub>Cl<sub>2</sub> (20 mL) and the protected dipyrromethane dialdehyde **2** (97 mg, 0.23 mmol), dissolved in dry CH<sub>2</sub>Cl<sub>2</sub> (5 mL), was added. The mixture was stirred at room temperature for 2 h under N<sub>2</sub> with exclusion of light. The resulting solution was then cooled in an ice bath and neutralized with triethylamine (362  $\mu$ L, 2.60 mmol). The mixture was diluted with dry CH<sub>2</sub>Cl<sub>2</sub> (30 mL) and extracted with brine (3  $\times$  50 mL). The evaporation of the solvent affords a dark residue, that was washed with pentane (10 mL). Yield 121 mg (76%). <sup>1</sup>H NMR (major tautomer, 200 MHz, CDCl<sub>3</sub>, 20  $^{\circ}$ C):  $\delta$  = 11.23, 10.70, 10.06 (br s; NH), 9.22 (s; H pyrrole), 8.40–7.50 (br s; NH), 8.10 (d; H phenyl), 7.44 (d; H phenyl), 6.85 (d; H pyrrole), 6.58 (s; meso-CH), 6.05 (d; H pyrrole), 5.93 (s; meso-CH), 5.63 (s; meso-CH), 4.41 (t; CH<sub>2</sub>CH<sub>2</sub>O), 4.1 (q; CH<sub>2</sub>CH<sub>3</sub>), 2.70–1.50 (m; CH<sub>2</sub>CH<sub>3</sub>, CH<sub>3</sub>), 1.12 (t; CH<sub>2</sub>CH<sub>2</sub>Si), 1.35 (m; CH<sub>2</sub>CH<sub>3</sub>), 0.082 ppm (s; Si(CH<sub>3</sub>)<sub>3</sub>); <sup>1</sup>H NMR (major tautomer, 200 MHz, CD<sub>3</sub>OD, 20  $^{\circ}$ C):  $\delta$  = 9.29 (s; H pyrrole), 9.23 (s; H pyrrole), 7.89 (d; H phenyl), 7.22 (d; H phenyl), 6.89 (d; H pyrrole), 6.63 (s; meso-CH), 5.90 (d; H pyrrole), 5.60, 5.44, 5.40 (s; meso-CH), 4.33 (t; CH<sub>2</sub>CH<sub>2</sub>O), 3.16 (q; CH<sub>2</sub>CH<sub>3</sub>), 1.26 (s; CH<sub>3</sub>), 1.04 (t; CH<sub>2</sub>CH<sub>2</sub>Si), 0.78 (t; CH<sub>2</sub>CH<sub>3</sub>), –0.006 ppm (s; Si(CH<sub>3</sub>)<sub>3</sub>); UV–vis (CH<sub>2</sub>Cl<sub>2</sub>)  $\lambda_{max}$  (nm): 300 (log  $\epsilon$  = 4.16), 482 (log  $\epsilon$  = 4.21), 802 (log  $\epsilon$  = 3.93); MS (ESI, positive mode, CH<sub>3</sub>OH):  $m/z$  696 ([MH]<sup>+</sup>), 714 ([MH + H<sub>2</sub>O]<sup>+</sup>), 728 ([MH + CH<sub>3</sub>OH]<sup>+</sup>).

#### 4.2.2. Synthesis of PCRed **4**

100 mg (0.25 mmol) of the tripyrrane diacid **1** was dissolved in 200  $\mu$ L (2.60 mmol) of TFA and kept under stirring for 10 min at room temperature under N<sub>2</sub>. The mixture was diluted with dry CH<sub>2</sub>Cl<sub>2</sub> (20 mL) and the protected dipyrromethane dialdehyde **2**

(97 mg, 0.23 mmol), dissolved in dry  $\text{CH}_2\text{Cl}_2$  (5 mL), was added. The mixture was stirred at room temperature for 2 h under  $\text{N}_2$  with exclusion of light. The resulting solution was then cooled in an ice bath and neutralized with triethylamine (362  $\mu\text{L}$ , 2.60 mmol). DDQ (2,3-Dichloro-5,6-Dicyanobenzoquinone, 105 mg, 0.46 mmol) was added and the ice bath removed. The mixture was stirred for 30 min at room temperature, diluted with dry  $\text{CH}_2\text{Cl}_2$  (30 mL) and extracted with brine ( $3 \times 50$  mL). Evaporation of the solvent affords a dark metallic green film. The residue was purified by flash chromatography (VersaFlash). Yield 80 mg (50%).  $^1\text{H NMR}$  (200 MHz,  $\text{CDCl}_3$ , 20 °C):  $\delta = 11.40$  (br s, 1H; NH), 10.21 (br s, 1H; NH), 9.27 (s, 2H; H pyrrole), 8.80–8.10 (br s, 2H; NH), 8.01 (d, 2H; H phenyl), 7.33 (d, 2H; H phenyl), 7.26 (s, 1H; meso-CH), 6.86 (d, 2H; H pyrrole), 6.05 (d, 2H; H pyrrole), 5.62 (s, 1H; meso-CH), 4.41 (t, 2H;  $\text{CH}_2\text{CH}_2\text{O}$ ), 3.12 (q, 4H;  $\text{CH}_2\text{CH}_3$ ), 1.25 (s, 6H;  $\text{CH}_3$ ),  $\text{CH}_2\text{CH}_2\text{Si}$ , 0.88 (t, 6H;  $\text{CH}_2\text{CH}_3$ ), 0.08 ppm (s, 9H;  $\text{Si}(\text{CH}_3)_3$ );  $^1\text{H NMR}$  (200 MHz,  $\text{CD}_3\text{OD}$ , 20 °C):  $\delta = 9.28$  (s, 2H; H pyrrole), 7.88 (d, 2H; H phenyl), 7.21 (d, 2H; H phenyl), 6.88 (d, 2H; H pyrrole), 6.52 (s, 2H; meso-CH), 5.90 (d, 2H; H pyrrole), 5.60 (s, 2H; meso-CH), 4.32 (t, 2H;  $\text{CH}_2\text{CH}_2\text{O}$ ), 3.16 (q, 4H;  $\text{CH}_2\text{CH}_3$ ), 1.23 (t, 6H;  $\text{CH}_2\text{CH}_3$ ), 1.20 (s, 6H;  $\text{CH}_3$ ), 1.04 (t, 2H;  $\text{CH}_2\text{CH}_2\text{Si}$ ),  $-\text{0.009}$  ppm (s, 9H;  $\text{Si}(\text{CH}_3)_3$ ); UV–vis ( $\text{CH}_2\text{Cl}_2$ )  $\lambda_{\text{max}}$  (nm): 485 (log  $\epsilon = 4.39$ ), 814 (log  $\epsilon = 3.71$ ); MS (ESI, positive mode,  $\text{CH}_3\text{OH}$ ):  $m/z$  694 ( $[\text{MH}]^+$ ), 726 ( $[\text{MH} + \text{CH}_3\text{OH}]^+$ ).

#### 4.2.3. Synthesis of Zn(II)-PCRed 5

a) Partially oxidized pentaporphynogen **3** (50 mg, 0.072 mmol) was dissolved in dry  $\text{CHCl}_3$  (70 mL) and stirred at room temperature for 30 min. A solution of anhydrous zinc acetate (60 mg, 0.33 mmol) and anhydrous sodium acetate (86 mg, 1.05 mmol) in methanol (5 mL) was added, and the mixture was stirred at room temperature for 48 h with exclusion of light.  $\text{CHCl}_3$  (70 mL) was added, and the solution was washed with deionized water ( $3 \times 20$  mL), dried over anhydrous sodium sulphate and evaporated at room temperature in vacuo. The residue was dissolved in acetone (2 mL), addition of *n*-pentane (10 mL) afforded a red-dark precipitate which was filtered and dried under reduced pressure. Yield 44 mg (81%). b) The preparation of **5** was carried out in a way similar to that described in the method a, using compound **4** (20 mg, 0.029 mmol) instead of **3**, and stirring the reaction mixture at room temperature only for 24 h. Yield 14 mg (64%).  $^1\text{H NMR}$  (200 MHz,  $\text{CDCl}_3$ , 20 °C):  $\delta = 10.03$  (br s, 1H; NH), 9.26 (s, 2H; H pyrrole), 9.0–7.0 (br s, 2H; NH), 8.02 (d, 2H; H phenyl), 7.97 (s, 1H; meso-CH), 7.28 (d, 2H; H phenyl), 6.86 (d, 2H; H pyrrole), 6.04 (d, 2H; H pyrrole), 5.58 (s, 1H; meso-CH), 4.45 (t, 2H;  $\text{CH}_2\text{CH}_2\text{O}$ ), 4.10 (q, 4H;  $\text{CH}_2\text{CH}_3$ ), 2.05 (s, 6H;  $\text{CH}_3$ ), 1.43 (t, 2H;  $\text{CH}_2\text{CH}_2\text{Si}$ ), 1.21 (t, 6H;  $\text{CH}_2\text{CH}_3$ ), 0.07 ppm (s, 9H;  $\text{Si}(\text{CH}_3)_3$ );  $^1\text{H NMR}$  (200 MHz,  $\text{CD}_3\text{OD}$ , 20 °C):  $\delta = 9.29$  (s, 2H; H pyrrole), 7.89 (d, 2H; H phenyl), 7.85 (s, 2H; meso-CH), 7.22 (d, 2H; H phenyl), 6.89 (d, 2H; H pyrrole), 5.90 (d, 2H; H pyrrole), 5.60 (s, 2H; meso-CH), 4.33 (t, 2H;  $\text{CH}_2\text{CH}_2\text{O}$ ), 4.01 (q, 4H;  $\text{CH}_2\text{CH}_3$ ), 1.92 (s, 6H;  $\text{CH}_3$ ), 1.15 (t, 6H;  $\text{CH}_2\text{CH}_3$ ), 1.04 (t, 2H;  $\text{CH}_2\text{CH}_2\text{Si}$ ),  $-\text{0.006}$  ppm (s, 9H;  $\text{Si}(\text{CH}_3)_3$ ); UV–vis ( $\text{CH}_2\text{Cl}_2$ )  $\lambda_{\text{max}}$  (nm): 407 (log  $\epsilon = 4.13$ ), 491 (log  $\epsilon = 4.33$ ), 817 (log  $\epsilon = 3.37$ ); MS (ESI, positive mode,  $\text{CH}_3\text{OH}$ ):  $m/z$  756 ( $[\text{M}]^+$ ), 774 ( $[\text{M} + \text{H}_2\text{O}]^+$ ), 788 ( $[\text{M} + \text{CH}_3\text{OH}]^+$ ).

#### 4.2.4. Synthesis of Lu(III)-PCRed 6

Partially oxidized pentaporphynogen **3** (40 mg, 0.057 mmol) was dissolved in dry  $\text{CHCl}_3$  (60 mL) and stirred at room temperature for 30 min. A solution of  $\text{Lu}(\text{OAc})_3 \cdot 4\text{H}_2\text{O}$  (110 mg, 0.257 mmol) and anhydrous sodium acetate (68 mg, 0.829 mmol) in methanol (8 mL) was added, and the mixture was stirred at room temperature for 72 h with exclusion of light.  $\text{CHCl}_3$  (60 mL) was added, and the solution was washed with deionized water ( $3 \times 20$  mL), dried over anhydrous sodium sulphate and evaporated at room temperature

in vacuo. The residue was dissolved in acetone (2 mL), addition of *n*-pentane (10 mL) afforded a red-dark precipitate which was filtered and dried under reduced pressure. Yield 44 mg (81%).  $^1\text{H NMR}$  (200 MHz,  $\text{CDCl}_3$ , 20 °C):  $\delta = 9.83$  (br s, 1H; NH), 9.31 (s, 2H; H pyrrole), 8.00 (d, 2H; H phenyl), 7.99 (s, 2H; meso-CH), 7.27 (d, 2H; H phenyl), 6.88 (d, 2H; H pyrrole), 6.06 (d, 2H; H pyrrole), 5.57 (s, 2H; meso-CH), 4.51 (q, 4H;  $\text{CH}_2\text{CH}_3$ ), 4.42 (t, 2H;  $\text{CH}_2\text{CH}_2\text{O}$ ), 1.26 (s, 6H;  $\text{CH}_3$ ), 1.12 (t, 2H;  $\text{CH}_2\text{CH}_2\text{Si}$ ), 0.84 (t, 6H;  $\text{CH}_2\text{CH}_3$ ), 0.075 ppm (s, 9H;  $\text{Si}(\text{CH}_3)_3$ );  $^1\text{H NMR}$  (200 MHz,  $\text{CD}_3\text{OD}$ , 20 °C):  $\delta = 9.29$  (s, 2H; H pyrrole), 7.89 (d, 2H; H phenyl), 7.81 (s, 2H; meso-CH), 7.21 (d, 2H; H phenyl), 6.88 (d, 2H; H pyrrole), 5.90 (d, 2H; H pyrrole), 5.60 (s, 2H; meso-CH), 4.32 (t, 2H;  $\text{CH}_2\text{CH}_2\text{O}$ ), 3.23 (q, 4H;  $\text{CH}_2\text{CH}_3$ ), 1.20 (s, 6H;  $\text{CH}_3$ ), 1.04 (t, 2H;  $\text{CH}_2\text{CH}_2\text{Si}$ ), 0.81 (t, 6H;  $\text{CH}_2\text{CH}_3$ ),  $-\text{0.007}$  ppm (s, 9H;  $\text{Si}(\text{CH}_3)_3$ ); UV–vis ( $\text{CH}_2\text{Cl}_2$ )  $\lambda_{\text{max}}$  (nm): 339 nm (log  $\epsilon = 4.25$ ), 406 nm (log  $\epsilon = 4.15$ ), 498 nm (log  $\epsilon = 3.99$ ); MS (EI, 70 eV):  $m/z$  (%): 865 (3), 394 (100).

#### 4.3. Cell lines

The HeLa human cervical cancer and the HepG2 hepatic carcinoma cells were cultured in DMEM (high glucose); the B78-H1 amelanotic clone derived from the murine melanoma was cultured in DMEM (low glucose) and the MCF-7 human breast cancer cell line was cultured in RPMI. All media (CELBIO, Milan, Italy) contained 10% fetal calf serum and were supplemented with antibiotics Penicillin 100 U/ml, Streptomycin 100  $\mu\text{g}/\text{ml}$  and Glutamine 2 mM (CELBIO, Milan, Italy). All experiments were done using exponential growth phase cells.

#### 4.4. PDT treatment

Treatment with different PCReds was performed at dark for 24 h and followed from irradiation with metal halogen white lamp at an irradiance of 8  $\text{mW}/\text{cm}^2$  for 60 min.

#### 4.5. Determination of cell proliferation

The % of viable cells was determined by the resazurin assay following the manufacturer's instructions (Sigma). To reach exponential growth phase, defined cell densities were seeded in a 96 multiwell plate: HeLa 5000 cells/well; HepG2 7000 cells/well; B78-H1 5000 cells/well and MCF-7 7000 cell/well. Values were obtained by spectrofluorometer Spectra Max Gemini XS (Molecular Devices, Sunnyvale).

#### 4.6. ROS measurement

ROS levels were determined after PDT by incubating the cells in white medium DMEM (Biowhittaker LONZA) without serum for 30 min at 37 °C with 5  $\mu\text{M}$  of 5-(and 6)-chloromethyl-2',7'-dichlorodihydrofluorescein diacetate, acetyl ester CM– $\text{H}_2\text{DCFDA}$  (mixed isomers, C6827, Molecular Probes, Invitrogen). CM– $\text{H}_2\text{DCFDA}$  was metabolized by non-specific esterases to the non-fluorescence product, which was oxidized to the fluorescent product, DCF, by ROS [18]. Then, the cells were washed twice in PBS, trypsinized, resuspended in PBS and measured for the ROS content by FACS (FACScan, Becton Dickinson).

#### 4.7. Confocal microscopy

To study the uptake, B78-H1 cells were plated (density of  $1 \times 10^5$ ) on coverslips (diameter 24 mm) and after 24 h treated with **4**, **5** and **6** (15  $\mu\text{M}$ ) for other 24 h. The glasses were prepared. The cells were washed twice with PBS, fixed with 3% paraformaldehyde (PFA) in PBS for 20 min. After washing with 0.1 M glycine,

containing 0.02% sodium azide in PBS to remove PFA and Triton-X-100 (0.1% in PBS), the cells were incubated with Hoechst to stain the nuclei. The cells were analysed using a Leica TCSNT confocal laser scanning system on an inverted microscope DMIRBE (Leica Microsystems, Heidelberg, German). Green fluorescence was excited with 488 nm line Argon-Ion laser and detected with emission bandpass filters 500/530 nm.

#### 4.8. FACS analysis

The B78-H1 cells were seeded in a 6 wells/plate at density of  $3 \times 10^5$  cells. The treatment was performed with **4**, **5** and **6** at concentrations of 15  $\mu$ M for 24 h. Then the cells were harvested, resuspended in 0.5 ml of PBS and washed twice and analysed by a FACScan (Becton Dickinson, San Jose, USA) equipped with a single 488 nm argon laser. A minimum of 10,000 cells for sample was acquired in list mode and analysed using Cell Quest software. The signal of **4**, **5** and **6** was detected by FL1 in log scale.

#### Acknowledgements

This study was supported by the Italian Ministry of University and Scientific Research (PRIN 2007), FVG and PRISMA. We thank Dr. M. Zacchigna (University of Trieste) for fluorescence measurements.

#### Appendix. Supplementary data

Supplementary data associated with this article can be found in the online version, at doi:10.1016/j.ejmech.2010.12.007.

#### References

- [1] (a) J.L. Sessler, A.E. Vivian, D. Seidel, A.K. Burrell, M. Hoehner, T.D. Mody, A. Gebauer, S.J. Weghorn, V. Lynch, Actinide expanded porphyrin complexes, *Coord. Chem. Rev.* 216 (2001) 411–434; (b) S. Hannah, V. Lynch, D.M. Guldi, N. Gerasimchuk, C.L.B. MacDonald, D. Magda, J.L. Sessler, Late first-row transition-metal complexes of texaphyrin, *J. Am. Chem. Soc.* 124 (2002) 8416–8427; (c) S. Mori, S. Shimizu, R. Taniguchi, A. Osuka, Group 10 metal complexes of meso-aryl-substituted [26]hexaphyrins with a metal–carbon bond, *Inorg. Chem.* 44 (2005) 4127–4129; (d) L.A. Yatsunyk, N.V. Shokhirev, F.A. Walker, Magnetic resonance spectroscopic investigations of the electronic ground and excited states in strongly nonplanar iron(III) dodecasubstituted porphyrins, *Inorg. Chem.* 44 (2005) 2848–2866.
- [2] J.L. Sessler, J.M. Davis, Sapphyrins: versatile anion binding agents, *Acc. Chem. Res.* 34 (2001) 989–997.
- [3] J.L. Sessler, J.S. Weghorn, in: J.E. Baldwin, F.R.S. Magnus, P.D. Magnus (Eds.), *Expanded, Contracted & Isomeric Porphyrins*, Tetrahedron Organic Chemistry Series, vol. 15, Elsevier Science Ltd, 1997 (chapter 6 and references cited therein).
- [4] (a) J.L. Sessler, A.K. Burrell, Expanded porphyrins, *Top. Curr. Chem.* 161 (1992) 177–273; (b) V.W. Day, T.J. Marks, W.A. Wachter, Large metal ion-centered template reactions. Uranyl complex of cyclopentakis(2-iminoisindoline), *J. Am. Chem. Soc.* 97 (1975) 4519–4527; (c) J.L. Sessler, G. Hemmi, T.D. Mody, T. Murai, A.K. Burrell, S.W. Young, Texaphyrins – synthesis and applications, *Acc. Chem. Res.* 27 (1994) 43–50; (d) A.K. Burrell, M. Cyr, V. Lynch, J.L. Sessler, Nucleophilic-attack at the meso position of a uranyl sapphyrin complex, *J. Chem. Soc. Chem. Commun.* 24 (1991) 1710–1713; (e) A.K. Burrell, G. Hemmi, V. Lynch, J.L. Sessler, Uranylpentaphyrin – an actinide complex of an expanded porphyrin, *J. Am. Chem. Soc.* 113 (1991) 4690–4692; (f) J.L. Sessler, T.D. Mody, V. Lynch, Synthesis and X-ray characterization of a uranyl(VI) schiff-base complex derived from a 2:2 condensation product of 3,4-diethyl pyrrole-2,5-dicarbaldehyde and 1,2-diamino-4,5-dimethoxybenzene, *Inorg. Chem.* 31 (1992) 529–531; (g) V. Král, E.A. Brucker, G. Hemmi, J.L. Sessler, J. Kralova, H. Bose Jr., A nonionic water-soluble pentaphyrin derivative – synthesis and cytotoxicity, *Bioorg. Med. Chem.* 3 (1995) 573–578.
- [5] (a) J.L. Sessler, T. Morishima, V. Lynch, Rubyrin – a new hexapyrrolic expanded porphyrin, *Angew. Chem. Int. Ed. Engl.* 30 (1991) 977–980; (b) J.L. Sessler, S. Weghorn, V. Lynch, M.R. Johnson, Turcasarin, the largest expanded porphyrin to date, *Angew. Chem. Int. Ed. Engl.* 33 (1994) 1509–1512; (c) T. Wessel, B. Franck, M. Möller, U. Rodewald, M. Läge, Porphyrins with aromatic 26- $\pi$ -electron systems, *Angew. Chem. Int. Ed. Engl.* 32 (1993) 1148–1151 (and references therein); (d) K. Schaffner, E. Vogel, G. Jori, Porphycenes as photodynamic therapy agents, in: *Biological Effects of Light*, de Gruyter, Berlin, 1994, pp. 312–321 (and references therein).
- [6] D. Magda, R.A. Miller, J.L. Sessler, B.L. Iverson, Site-specific hydrolysis of RNA by europium(III) texaphyrin conjugated to a synthetic oligodeoxyribonucleotide, *J. Am. Chem. Soc.* 116 (1994) 7439–7440.
- [7] (a) C.J. Gomer, Photodynamic therapy in the treatment of malignancies, *Semin. Hematol.* 26 (1989) 27–34; (b) T.J. Dougherty, Hematoporphyrin as a photosensitizer of tumors, *Photochem. Photobiol.* 38 (1983) 377–379; (c) H.L. Pass, Photodynamic therapy in oncology – mechanisms and clinical use, *J. Natl. Cancer Inst.* 85 (1993) 443–456; (d) S.B. Brown, T.G. Truscott, New light on cancer therapy, *Chem. Brit.* 29 (1993) 955–958.
- [8] (a) R.R. Allison, V.S. Bagnato, C.H. Sibata, Future of oncologic photodynamic therapy, *Future Oncol.* 6 (2010) 929–940; (b) *Curr. Pharm. Des.* 16 (2010) 1863–1976; (c) A.D. Garg, D. Nowis, J. Golab, P. Agostinis, Photodynamic therapy: illuminating the road from cell death towards anti-tumor immunity, *Apoptosis* 15 (2010) 1050–1071; (d) M.C. Almeida Issa, M. Manela-Azulay, Photodynamic therapy: a review of the literature and image documentation, *Bras. Dermatol.* 85 (2010) 501–511; (e) S.O. Gollnick, C.M. Brackett, Enhancement of anti-tumor immunity by photodynamic therapy, *Immunol. Res.* 46 (2010) 216–226; (f) B. Ortel, C.R. Shea, P. Calzavara-Pinton, Molecular mechanisms of photodynamic therapy, *Front. Biosci.* 14 (2009) 4157–4172; (g) D.E. Dolmans, D. Fukumura, R.K. Jain, Photodynamic therapy for cancer, *Nat. Rev. Cancer* 3 (2003) 380–387; (h) C.H. Sibata, V.C. Colussi, N.L. Oleinick, T.J. Kinsella, Photodynamic therapy in oncology, *Expert Opin. Pharmacother.* 2 (2001) 917–927; (i) T.J. Dougherty, An update on photodynamic therapy applications, *J. Clin. Laser Med. Surg.* 20 (2002) 3–7.
- [9] (a) T.J. Dougherty, C.J. Gomer, B.W. Henderson, G. Jori, D. Kessel, M. Korbelik, J. Moan, Q. Peng, Photodynamic therapy, *J. Natl. Cancer Inst.* 90 (1998) 889–905; (b) J. Miller, Photodynamic therapy: the sensitization of cancer cells to light, *Chem. Educ. Today* 76 (1999) 592–594; (c) S. Pervaiz, Reactive oxygen-dependent production of novel photochemotherapeutic agents, *FASEB J.* 15 (2001) 612–617.
- [10] (a) L.B. Josefsen, R.W. Boyle, Photodynamic therapy and the development of metal-based photosensitizers, *Metal Based Drugs* (2008) Article ID 276109; (b) H. Ali, J.E. van Lier, Metal complexes as photo- and radio-sensitizers, *Chem. Rev.* 99 (1999) 2379–2450.
- [11] (a) C. Comuzzi, S. Cogoi, M. Overhand, G.A. Van der Marel, H.S. Overkleef, L.E. Xodo, Synthesis and biological evaluation of new pentaphyrin macrocycles for photodynamic therapy, *J. Med. Chem.* 49 (2006) 196–204; (b) C. Comuzzi, S. Cogoi, L.E. Xodo, Spectroscopic characterization of the oxidation control of the iso-pentaphyrin/pentaphyrin system, *Tetrahedron* 62 (2006) 8147–8151.
- [12] (a) D.J. Ball, S.R. Wood, D.I. Vernon, J. Griffiths, T.M.A.R. Dubbelman, S.B. Brown, The characterization of three substituted zinc phthalocyanines of differing charge for use in photodynamic therapy. A comparative study of their aggregation and photosensitising ability in relation to mTHPC and polyhaematoporphyrin, *J. Photochem. Photobiol. B.* 45 (1998) 28–35; (b) V. Mantareva, V. Kussovski, I. Angelov, E. Borisova, L. Avramov, G. Schnurpfeild, D. Wöhrled, Photodynamic activity of water-soluble phthalocyanine zinc(II) complexes against pathogenic microorganisms, *Bioorg. Med. Chem.* 15 (2007) 4829–4835.
- [13] D.M. Guldi, T.D. Mody, N.N. Gerasimchuk, D. Magda, J.L. Sessler, Influence of large metal cations on the photophysical properties of texaphyrin, a rigid aromatic chromophore, *J. Am. Chem. Soc.* 122 (2000) 8289–8298.
- [14] R.E. Danso-Danquah, L.Y. Xie, D. Dolphin, Characterization of decamethyl and ethoxycarbonyl pentaphyrins, *Heterocycles* 41 (1995) 2553–2564.
- [15] (a) Q.M. Huang, Z.Q. Pan, P. Wang, Z.P. Chen, X.L. Zhang, H.S. Xu, Zinc(II) and copper(II) complexes of  $\beta$ -substituted hydroxylporphyrins as tumor photosensitizers, *Bioorg. Med. Chem. Lett.* 16 (2006) 3030–3033; (b) J. Scott, J.M.E. Quirke, H.J. Vreman, D.K. Stevenson, K.R. Downum, Metalloporphyrin phototoxicity, *J. Photochem. Photobiol. B.* 7 (1990) 149–157.
- [16] (a) T.M. Busch, H.W. Wang, E.P. Wileto, G.Q. Yu, R.M. Bunte, Increasing damage to tumor blood vessels during motexafin Lutetium-PDT through use of low fluence rate, *Radiat. Res.* 174 (2010) 331–340; (b) A.E. O'Connor, W.M. Gallagher, A.T. Byrne, Porphyrin and nonporphyrin photosensitizers in oncology: preclinical and clinical advances in photodynamic therapy, *Photochem. Photobiol.* 85 (2009) 1053–1074; (c) K. Verigos, R. Mick, T.C. Zhu, R. Whittington, D. Smith, A. Dimofte, J. Finlay, T.M. Busch, Z.A. Tochner, S.B. Malkowicz, E. Glatstein, S.M. Hahn, Updated results of a phase I trial of motexafin lutetium-mediated interstitial photodynamic therapy in patients with locally recurrent prostate cancer, *J. Environ. Pathol. Tox.* 25 (2006) 373–387; (d) H.M. Ross, J.A. Smelstoy, G.J. Davis, A.S. Kapatkin, F. Del Piero, E. Reineke, H. Wang, T.C. Zhu, T.M. Busch, A.G. Yodh, S.M. Hahn, Photodynamic therapy with motexafin lutetium for rectal cancer: a preclinical model in the dog,

- J. Surg. Res. 135 (2006) 323–330;
- (e) T.C. Zhu, J.C. Finlay, S.M. Hahn, Determination of the distribution of light, optical properties, drug concentration, and tissue oxygenation in-vivo in human prostate during motexafin lutetium-mediated photodynamic therapy, *J. Photochem. Photobiol. B.* 79 (2005) 231–241.
- [17] (a) V. Král, H. Furuta, K. Shreder, V. Lynch, J.L. Sessler, Protonated sapphyrins, highly effective phosphate receptors, *J. Am. Chem. Soc.* 118 (1996) 1595–1607; (b) B.L. Iverson, K. Shreder, V. Král, P. Sansom, V. Lynch, J.L. Sessler, Interaction of sapphyrin with phosphorylated species of biological interest, *J. Am. Chem. Soc.* 118 (1996) 1608–1616; (c) N. Sheng, P.-H. Zhu, C.-Q. Ma, J.-Z. Jiang, The synthesis, spectroscopy, electrochemistry and photophysical properties of novel, sandwich europium(III) complexes with a porphyrin ligand bearing four pyrenyl groups in meso-positions, *Dyes Pigm.* 81 (2009) 91–96.
- [18] (a) T.L. Dawson, G.J. Gores, A.L. Nieminen, B. Herman, J.J. Lemasters, Mitochondria as a source of reactive oxygen species during reductive stress in rat hepatocytes, *Am. J. Physiol.* 264 (1993) C961–C967; (b) A.L. Nieminen, A.M. Byrne, B. Herman, J.J. Lemasters, Mitochondrial permeability transition in hepatocytes induced by t-BuOOH: NAD(P)H and reactive oxygen species, *Am. J. Physiol.* 272 (1997) C1286–C1294; (c) C.P. LeBel, H. Ischiropoulos, S.C. Bondy, Evaluation of the probe 2',7'-dichlorofluorescein as an indicator of reactive oxygen species formation and oxidative stress, *Chem. Res. Toxicol.* 5 (1992) 227–231; (d) R. Cathcart, E. Schwiers, B.N. Ames, Detection of picomole levels of hydroperoxides using a fluorescent dichlorofluorescein assay, *Anal. Biochem.* 134 (1983) 111–116; (e) R. Brandt, A.S. Keston, Synthesis of diacetyldichlorofluorescein – a stable reagent for fluorometric analysis, *Anal. Biochem.* 11 (1965) 6–9.
- [19] (a) C.A. Robertson, D. Hawkins Evans, H. Abrahamse, Photodynamic therapy (PDT): a short review on cellular mechanisms and cancer research applications for PDT, *J. Photochem. Photobiol. B. Biol.* 96 (2009) 1–8; (b) P. Mroz, A. Pawlak, M. Satti, H. Lee, T. Wharton, H. Gali, T. Sarna, M.R. Hamblin, Functionalized fullerenes mediate photodynamic killing of cancer cells: type I versus Type II photochemical mechanism, *Free Radic. Biol. Med.* 43 (2007) 711–719; (c) P. Bilski, A.G. Belanger, C.F. Chignell, Photosensitized oxidation of 2',7'-dichlorofluorescein: singlet oxygen does not contribute to the formation of fluorescent oxidation product 2',7'-dichlorofluorescein, *Free Radic. Biol. Med.* 33 (2002) 938–946.
- [20] E. Gross, B. Ehrenberg, F.M. Johnson, Singlet oxygen generation by porphyrins and the kinetics of 9,10-dimethylanthracene photosensitization in liposomes, *Photochem. Photobiol.* 57 (1993) 808–813.
- [21] (a) K.M. Barkigia, L. Chantranupong, K.M. Smith, J. Fajer, Structural and theoretical models of photosynthetic chromophores. Implications for redox, light-absorption properties and vectorial electron flow, *J. Am. Chem. Soc.* 110 (1988) 7566–7567; (b) A.K. Wertsching, A.S. Koch, S.G. DiMaggio, On the negligible impact of ruffling on the electronic spectra of porphine, tetramethylporphyrin, and perfluoroalkylporphyrins, *J. Am. Chem. Soc.* 123 (2001) 3932–3939; (c) H. Ryeng, A. Ghosh, Do nonplanar distortions of porphyrins bring about strongly red-shifted electronic spectra? Controversy, consensus, new developments, and relevance to chelatases, *J. Am. Chem. Soc.* 124 (2002) 8099–8103; (d) R.E. Haddad, S. Gazeau, J. Pecaut, J.-C. Marchon, C.J. Medforth, J.A. Shelnutt, Origin of the red shifts in the optical absorption bands of nonplanar tetraalkylporphyrins, *J. Am. Chem. Soc.* 125 (2003) 1253–1268.
- [22] (a) J.-Y. Shin, H. Furuta, A. Osuka, N-fused pentaphyrin, *Angew. Chem. Int. Ed.* 40 (2001) 619–621; (b) A. Krivokapic, A.R. Cowley, H.L. Anderson, Contracted and expanded meso-alkynyl porphyrinoids: from triphyrin to hexaphyrin, *J. Org. Chem.* 68 (2003) 1089–1096.